

Solute transport and storage mechanisms in wetlands of the Everglades, south Florida

Judson W. Harvey

U.S. Geological Survey, Reston, Virginia, USA

James E. Saiers

School of Environmental Studies, Yale University, New Haven, Connecticut, USA

Jessica T. Newlin

U.S. Geological Survey, Reston, Virginia, USA

Received 20 July 2004; revised 18 January 2005; accepted 4 February 2005; published 12 May 2005.

[1] Solute transport and storage processes in wetlands play an important role in biogeochemical cycling and in wetland water quality functions. In the wetlands of the Everglades, there are few data or guidelines to characterize transport through the heterogeneous flow environment. Our goal was to conduct a tracer study to help quantify solute exchange between the relatively fast flowing water in the open part of the water column and much more slowly moving water in thick floating vegetation and in the pore water of the underlying peat. We performed a tracer experiment that consisted of a constant-rate injection of a sodium bromide (NaBr) solution for 22 hours into a 3 m wide, open-ended flume channel in Everglades National Park. Arrival of the bromide tracer was monitored at an array of surface water and subsurface samplers for 48 hours at a distance of 6.8 m downstream of the injection. A one-dimensional transport model was used in combination with an optimization code to identify the values of transport parameters that best explained the tracer observations. Parameters included dimensions and mass transfer coefficients describing exchange with both short (hours) and longer (tens of hours) storage zones as well as the average rates of advection and longitudinal dispersion in the open part of the water column (referred to as the “main flow zone”). Comparison with a more detailed set of tracer measurements tested how well the model’s storage zones approximated the average characteristics of tracer movement into and out of the layer of thick floating vegetation and the pore water in the underlying peat. The rate at which the relatively fast moving water in the open water column was exchanged with slowly moving water in the layer of floating vegetation and in sediment pore water amounted to 50 and 3% h^{-1} , respectively. Storage processes decreased the depth-averaged velocity of surface water by 50% relative to the water velocity in the open part of the water column. As a result, flow measurements made with other methods that only work in the open part of the water column (e.g., acoustic Doppler) would have overestimated the true depth-averaged velocity by a factor of 2. We hypothesize that solute exchange and storage in zones of floating vegetation and peat pore water increase contact time of solutes with biogeochemically active surfaces in this heterogeneous wetland environment.

Citation: Harvey, J. W., J. E. Saiers, and J. T. Newlin (2005), Solute transport and storage mechanisms in wetlands of the Everglades, south Florida, *Water Resour. Res.*, 41, W05009, doi:10.1029/2004WR003507.

1. Introduction

[2] Solute transport in wetlands is a key pathway for the movement of materials and cycling of carbon, nutrients, and energy. Hydrologic transport processes influence the rate of delivery of reactants and the rate of flushing of products from sites where specific chemical reactions are favored [McClain *et al.*, 2003]. Of particular interest in wetlands is

water exchange between areas of relatively fast flowing surface water and areas of slower moving waters, such as water within zones of thick submerged aquatic vegetation and pore water in the sediment. Repeated exchange of water and solute between the open part of the surface water column where downstream flow occurs (referred to as the “main flow zone”), and zones of stagnant or very slow flow in areas of thick vegetation and within peat sediment (“storage zones”), have significant potential to influence downstream water quality. This is because the average velocity with which solutes move downstream is decreased,



Figure 1. Photograph from the head of experimental flume facility “A” in Everglades National Park looking south toward the flume outlet (100 m away). Three of these flume facilities were constructed in the park by scientists at Florida International University. Each flume consists of four open-ended channels divided by plastic walls and floating walkways. Our tracer experiment was conducted in the easternmost channel (right side of photo) by injecting a solution of NaBr at a constant rate near the upstream edge of vegetation. Four horizontal soaker hoses distributed the tracer evenly across the channel and with depth in the 60 cm water column. The breakthrough of Br tracer was measured at a distance of 6.8 m downstream over a period of 48 hours. Sampling consisted of the pumping of small-volume water samples at seven locations in surface water and seven locations in the subsurface (peat) pore water in the measurement cross section (see Figure 2) (photo provided by Florida International University).

allowing more contact time for reactions, and because biogeochemical reactions are stimulated as a result of close contact with microbially and geochemically reactive coatings on vegetation and sediment particles [Jones and Mulholland, 2000].

[3] A challenge for wetland researchers is detecting and quantifying solute exchange between the relatively fast and slow flowing parts of these heterogeneous systems. One approach that has not been frequently attempted in wetlands is the injection and detailed monitoring of the movement of solute tracers. Often used successfully in streams, the tracer approach quantifies processes in a way that recognizes the need to characterize the average characteristics of transport and storage (rather than characterizing individually a multitude of flow paths). For example, tracer analysis in streams can supply average “reach-scale” characteristics of surface and subsurface flow, and, if care is taken in sampling, tracer analysis can further discriminate between the relative contributions of different components of the flow system (e.g., pools and eddies, streambed periphyton, streambed gravel deposits, and near stream alluvium) [Harvey and Fuller, 1998; Gooseff *et al.*, 2004]. The goal of the present paper was to use a tracer-based approach to characterize the major components of solute flow and transport in the heterogeneous wetland system of the Everglades.

[4] Field-based measurements of solute transport in wetlands are relatively few [Nepf, 1997, 1999; Andradottir and Nepf, 2001; Martinez and Wise, 2003; Keefe *et al.*, 2004].

Most previous tracer experiments in wetlands have taken place either in coastal systems [Harvey *et al.*, 1995; Nepf, 1999; Tobias *et al.*, 2001], or in wetlands constructed for water treatment [Schulz and Peall, 2001; Martinez and Wise, 2003; Keefe *et al.*, 2004]. A rich literature does exist in the performance of wetlands constructed for water treatment [e.g., Kadlec and Knight, 1996]; however, many of those investigations are based on comparisons of chemistry in the input and output waters of the wetlands, with relatively little emphasis on the solute transport processes themselves. It is also worth noting that most constructed wetlands differ considerably in plant species composition, nutrient status, and generally experience higher average velocities than do less disturbed wetlands such as the Everglades.

[5] The Everglades is a very large (8×10^5 hectares) peatland in south Florida vegetated with emergent and submerged macrophytes that are tolerant of the naturally low nutrient conditions. Depending on location, the wetlands are inundated either seasonally or perennially by a combination of local rainfall, overflow from Lake Okeechobee, drainage from surrounding uplands, and groundwater discharge [National Research Council, 2003]. Surface water in the Everglades flows in a generally southerly or southwesterly direction through the grasses and other macrophytes at relatively low velocities that generally range between 0.5 and 2.0 cm s^{-1} [Riscassi and Schaffranek, 2003]. Flow from the Everglades is then discharged to

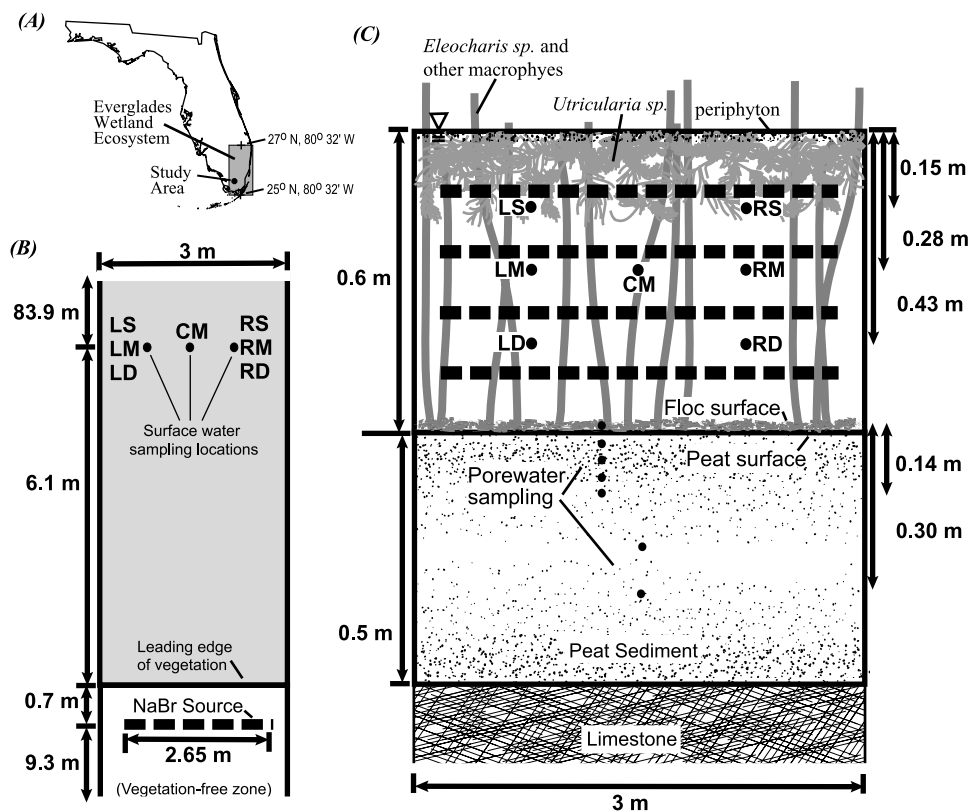


Figure 2. (a) Map showing general location of tracer study in southern Everglades, south Florida. (b) Plan view showing locations of the tracer injection source and surface water sampling tubes in the experimental channel. (c) Cross section showing positions of the tracer injection soaker hoses (dashed lines), surface and subsurface water sampling tubes, and layers of vegetation, viewed looking downstream from the head of the channel.

coastal bays and to the Gulf of Mexico near the southern tip of Florida.

[6] Relatively few solute tracer experiments have been conducted in naturally slow flowing and nutrient poor wetlands such as the Everglades. Our tracer experiment was conducted in an experimental flume facility operated by Florida International University in Everglades National Park located in the southernmost part of the Everglades (Figures 1 and 2a). Rates of advection and longitudinal dispersion in surface water were quantified, as well as rates of solute exchange between main flow zones in surface water and much more slowly flowing water in dense floating vegetation and in peat pore water. The average size and average fluid residence times in these “storage zones” were quantified, as was the overall effect of storage in retarding downstream movement of solutes. These results have implications for the fate and transport of important surface water contaminants during transport through the Everglades wetland ecosystem, including the fate of phosphorus [Noe *et al.*, 2002], mercury [Krabbenhoft *et al.*, 1998], and sulfate [Bates *et al.*, 2002].

2. Site Description

[7] The tracer experiment was conducted in Shark River Slough, which is the main surface water drainage way in Everglades National Park that delivers freshwater flow from

the central Everglades to coastal waters in Whitewater Bay and the Gulf of Mexico. The experiment was conducted in flume “A” (25°38′31.2″N, 80°43′20.4″W), which is one of the three flumes in the park managed by researchers at Florida International University (Figures 1 and 2). The flume facility is oriented parallel to the average flow direction and consists of four side-by-side channels, each 3.0 m wide, extending for 100 m in a southerly direction. The channels remain open at both ends, which allows Everglades surface water to flow through the channels at ambient rates. Plastic sidewalls and floating walkways keep the water in the individual channels separated, and allow access to measurement points without disturbance to flow or to the peat sediment. Other details on the construction, operation, and results from flume research are given by Noe *et al.* [2002]. Our injection was conducted on 20 November 2002 in the westernmost channel of the flume (Figures 1 and 2b). Surface water was 60 cm deep at the time of the experiment, and a typical assemblage of Everglades slough vegetation was present (Figure 2c). Emergent macrophytes were dominated by the rooted *Eleocharis cellulosa* (806 stems m⁻²) and *Eleocharis elongata* (341 stems m⁻²), while several species of submerged aquatic plants were dominated by *Utricularia purpurea* and *Utricularia foliosa*. The submerged macrophytes floated beneath the water surface in a layer that was 20 cm thick at the time of the experiment. Periphyton (a matrix of algae and heterotrophic

microbes) was also present as a mat floating in the top 2 cm of the water column, and also as thin coatings (“sweaters”) on *Eleocharis* stems. At the sediment surface is a layer of flocculent organic detritus (referred to as “floc”) that was approximately 3 cm thick at the time of the experiment. Beneath the floc is peat, which is similar in constitution to floc but is finer grained and more consolidated. The rooted macrophytes are anchored in the peat, which is approximately 50 cm in thickness and underlain by limestone at the location of the experiment. There are few published data describing physical and hydrological characteristics of Everglades peat. Recent measurements from the experimental flume suggest that Everglades floc and peat typically have bulk densities of 0.01 and 0.06 g cm⁻³, respectively, and porosities of 0.99 and 0.88, respectively [Jones *et al.*, 1999]. Similar peat in the interior of Water Conservation Area 2A in the central Everglades had a hydraulic conductivity of 7×10^{-4} cm s⁻¹ [Harvey *et al.*, 2004]. No measurements of hydraulic conductivity are available for Everglades floc, although it is reasonable to expect (given its lower bulk density and higher porosity compared with peat) that the hydraulic conductivity of floc is greater.

3. Tracer Experimental Design and Methodology

[8] The injection consisted of the steady, 22 hr injection (at 100 mL min⁻¹) of a sodium bromide (NaBr) solution that had been dissolved in Everglades water that was filtered (0.2 μm) on site. Bromide was used as the solute tracer because of its conservative nature in Everglades water with circumneutral pH and a very low background concentration of Br (0.05 mg L⁻¹). The injection took place at a distance of 0.75 m upgradient of the upstream edge of vegetation in the experimental channel (Figure 2b). The tracer was introduced uniformly with depth and width across the channel by dividing the injection stream between four horizontally oriented soaker hoses (2.65 m long) that were spaced evenly with depth in the water column (Figure 2c). The distribution of the bromide tracer over the full depth of the surface water column distinguishes the design of this experiment from that of a companion experiment in which microscopic particles composed of TiO₂ were injected through a single soaker hose [Saiers *et al.*, 2003].

[9] Bromide tracer concentration was monitored at a distance 6.8 m downstream of the injection beginning at the start of the injection and continuing for 48 hrs. Small-volume (10 mL) water samples were collected in 20 mL plastic scintillation vials for Br analysis by applying suction to 1/8 inch stainless steel sampling tubes deployed throughout the water column and in the peat sediment to a depth of 30 cm. In surface water, the sampling tubes are designated as LS, LM, LD, CM, RS, RM, and RD, where L (left), C (center), and R (right) delineate lateral position in the channel (looking downstream) and refer to locations 0.9 m inside the left wall, at the channel center, and 0.9 m inside the right wall, respectively, and S (shallow), M (middepth), and D (deep) delineate vertical position and refer to depths of 15, 27.5, and 42.5 cm below the water surface, respectively (Figure 2c).

[10] Sampling tubes were also deployed in the peat sediment. These tubes were used to sample pore water of the floc (3 cm thick layer) and in the peat beneath the floc (approximately a 50 cm thick layer). Pore water was

sampled from the following depths: 1.8, 4.3, 6.8, 9.3, 11.8, 20, and 30 cm below the surface of the floc layer (Figure 2c). Pore water sampling was conducted by very slow peristaltic pumping (1.5 mL min) using a multi-channel pump head following the design of Duff *et al.* [1998]. After the tracer experiment was completed, bromide concentrations in all samples were measured in the laboratory by ion chromatography with a detection limit of 0.02 mg L⁻¹, which easily allowed tracer concentrations to be distinguished from background concentrations of Br in surface water (0.05 mg L⁻¹) and in deeper pore water (0.18 mg L⁻¹).

4. Modeling

4.1. Analysis Equations

[11] An extended version of the one-dimensional solute transport model by Runkel [1998], developed by Choi *et al.* [2000], was used to characterize the results of tracer experiments. We refer to our modified version of OTIS-P as the OTIS-2stor module. The governing equations are

$$\frac{\partial C}{\partial t} = -\frac{Q}{A} \frac{\partial C}{\partial x} + \frac{1}{A} \frac{\partial}{\partial x} \left(AD_L \frac{\partial C}{\partial x} \right) + \frac{q_L^{in}}{A} (C_L - C) + \alpha_1 (C_{S1} - C) + \alpha_2 (C_{S2} - C), \quad (1)$$

$$\frac{dC_{S1}}{dt} = \alpha_1 \frac{A}{A_{S1}} (C - C_{S1}), \quad (2)$$

$$\frac{dC_{S2}}{dt} = \alpha_2 \frac{A}{A_{S2}} (C - C_{S2}), \quad (3)$$

where

C	main channel solute concentration [mg L ⁻¹];
Q	volumetric flow rate [m ³ s ⁻¹];
A	main flow zone cross-sectional area [m ²];
D_L	longitudinal dispersion coefficient [m ² s ⁻¹];
q_L^{in}	lateral inflow rate [m ³ s ⁻¹ m ⁻¹];
q_L^{out}	lateral outflow rate [m ³ s ⁻¹ m ⁻¹];
C_L	lateral inflow solute concentration [mg l ⁻¹];
α_1	storage zone 1 exchange coefficient [s ⁻¹];
C_{S1}	storage zone 1 solute concentration [mg L ⁻¹];
A_{S1}	storage zone 1 cross-sectional area [m ²];
α_2	storage zone 2 exchange coefficient [s ⁻¹];
C_{S2}	storage zone 2 solute concentration [mg L ⁻¹];
A_{S2}	storage zone 2 cross-sectional area [m ²];
t	time [s];
x	distance [m].

[12] The governing equations of the OTIS-2stor module were solved by modifying the USGS numerical code OTIS-P (One-dimensional Transport with Inflow and Storage with Parameter Estimation) [Runkel, 1998] to solve the extended governing equations for a flow system with two-storage zones. Since the model extension is not the primary contribution of the present paper, the conceptual basis of the model is only briefly reviewed here. The reader is referred to Choi *et al.* [2000], Harvey and Wagner [2000], and Runkel [1998] for more detailed discussions of the model’s conceptual basis, its relation to earlier

models, and solution techniques. A thorough documentation of the OTIS-2Stor module is in preparation.

[13] Both the OTIS-2stor module and its predecessor are often used for the analysis of tracer experiments by applying them in the inverses sense, i.e., model parameters are adjusted using statistical optimization to determine the values of the parameters that best simulate the measured tracer data. Average velocity and cross sectional area of flow are two of the primary parameters of interest. Both a mean velocity, V , and an associated cross sectional area, A , are identified through optimization of the parameters of the model. Typically the modeling shows that not all parts of the water column participate in downstream advection, due to the existence of zones with stagnant or very slowly flowing water referred to as “storage” zones. The zone with cross sectional area A is therefore typically smaller than measurements of the total cross sectional area of surface water. We therefore refer the modeled zone where downstream advection occurs as the “main flow zone” in order to distinguish it from the total cross sectional area.

[14] In addition to quantifying advection we were also interested in quantifying parameters that describe longitudinal mixing of solutes. The first of those is the longitudinal dispersion parameter, D_L , which characterizes the relatively fast components of mixing that arise due to velocity variations in the main flow zone. To be characterized by the longitudinal dispersion parameter, mixing processes must achieve equilibrium (i.e., all tracer must experience the full range of flow velocities in the main flow zone) during the tracer experiment. Slower processes of longitudinal mixing are better characterized as “storage exchange.” Conceptually, storage is the result of water being exchanged between the main flow zone and “storage zones,” where water is stagnant or very slow moving relative to the main flow zone. The storage parameters α and A_s characterize these slower components of mixing that do not achieve a state of equilibrium mixing during the experiment [Harvey and Wagner, 2000]. The residence time distribution for fluid and solute entering the storage zone is exponential, with an average residence time equal to $A_s/(\alpha A)$. An additional parameter of interest is the depth-averaged velocity of tracer, V' , which is slower than velocity in the main flow zone. Depth-averaged velocity can be estimated from the model-estimated parameters as $V \cdot A/(A + A_s)$ where V is the velocity for the main flow zone, while A and A_s are the cross sectional areas of the main flow zone and storage zone, respectively.

[15] Using two storage zones instead of just one as prescribed by Choi *et al.* [2000] allows a broader range of storage timescales to be characterized, due to the model’s inclusion of a second storage zone with a different (usually a much longer) mean residence time. Therefore, for the two-storage model there are four storage parameters (α_1 , A_{s2} , α_2 , and A_{s2}) that must be estimated to characterize exchange between the main flow zone and storage environments. Each storage zone has a unique fluid residence time, $A_{s1}/(\alpha_1 A)$ and $A_{s2}/(\alpha_2 A)$. Also, V' is now calculated as $V \cdot A/(A + A_{s1} + A_{s2})$ where A_{s1} and A_{s2} are the cross sectional areas of storage zones 1 and 2, respectively.

4.2. Approach for Estimating Model Parameters

[16] Our purpose in using the two-storage-zone model was to test the hypothesis that the major mechanisms of

storage in the Everglades wetlands could be identified and quantified through tracer experimentation and inverse modeling. We anticipated that the mixing that resulted from velocity variations within the macrophyte stems would be characterized by the longitudinal dispersion parameter, while mixing that resulted by exchange between the main flow zone and zones of much more slowly moving water in floating vegetation and in peat pore water could be characterized by the two storage zones, respectively.

[17] The volumetric flow rate of surface water in the channel (Q) and inflow and outflow fluxes (q_L^{in} , q_L^{out}) were calculated using estimates of (1) injection pumping rate, (2) Br concentration in the injection solution barrel, (3) background concentration of Br tracer, and (4) concentrations of Br in surface water during the injection a short distance downstream of the injection and at a distance of 6.8 m. All of the other parameters were estimated by the nonlinear least squares optimization described previously. The optimized parameters included, depending on the particular simulation, A , D_L , A_{s1} , and A_{s2} , and exchange coefficients, α_1 and α_2 . Model runs began at the start of the injection, but, due to practical and theoretical reasons, only tracer measurements during the last 4 hours of the tracer plateau and the 27 hours following the end of the injection (i.e., the tail of the breakthrough curve) were used for parameter calibration. The reason was that the background tracer concentration is known with considerably more certainty compared with the plateau tracer concentration. As a consequence, the task of estimating storage parameters on the tail of the experiment (compared with on the rising limb of the experiment) is more reliable. Note that this argument only applies if a plateau tracer concentration is reached during the experiment, because that condition allows volumetric flow rate and inflow to be calculated independently of the model optimization. If volumetric flow rate and inflow are not known from plateau tracer data (as is typical for a “pulse” tracer breakthrough that never achieves plateau), then all the data from the rising and falling limb of the tracer experiment must be used in the statistical optimization.

4.3. Optimization and Uncertainty of Estimated Parameters

[18] The “best fit” values of the transport parameters were estimated by an inverse approach that uses generalized nonlinear least squares, together with other statistical criteria, to objectively search for a set of parameters that minimize the differences between model calculations and observations. An optimization routine that has frequently been used in the past for that purpose is called STARPAC [Donaldson and Tryon, 1990]. Its use with stream tracer applications is thoroughly documented by Wagner and Harvey [1997], Runkel [1998], and Harvey and Wagner [2000]. The reliability of the parameter values that result from optimization are a function of several criteria. First is the choice of the objective function itself (along with other quantitative criteria that help determine whether convergence on a solution has occurred). STARPAC uses a formulation of the residual sum of squares (RSS) which can be weighted (to account for unequal variances associated with observations). This weighting scheme treats the problem of unequal variances of observations across the full range of values of the tracer observations, which helps to emphasize the valuable information about storage paramete-

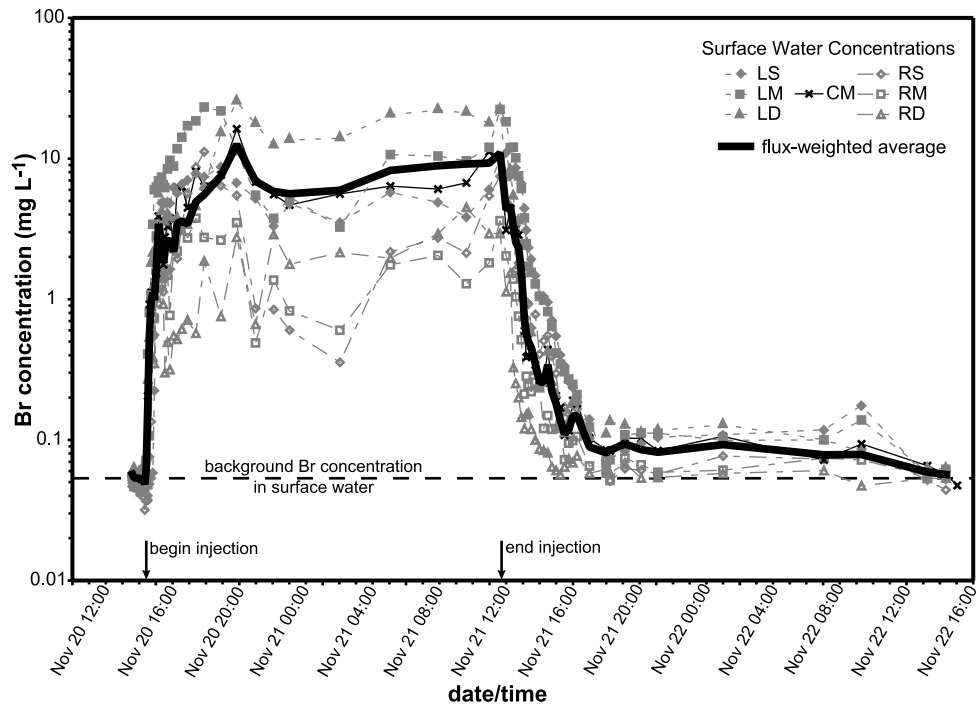


Figure 3. Observed (symbols and dashed lines) and averaged (thick solid line) concentrations of Br tracer during the 2 day tracer experiment. Observed concentrations are referenced to the lateral and vertical positions of the sampling tubes (Figure 2c). Averaged concentrations are flux weighted (see text for explanation). Start and end times of the injection are shown as arrows on the ordinate.

ters contained within the lowest magnitude concentrations on the tail of the breakthrough curve [Wagner and Harvey, 1997]. To make the test for convergence even more rigorous, we always use the established convention of changing the values of the starting parameters and rerunning even the models that successfully converged to ensure that resulting parameter estimates are not affected by choice of starting parameter values. A second important indicator of the reliability of parameters determined by inverse modeling is the standard deviations (reported here as coefficients of variation) that are associated with the estimation of the “optimal” parameter values. These uncertainties are a function of the sensitivity of the model output with respect to changes in the parameter values, as well as the number of data collected and assumptions about the precision of those data [Wagner and Harvey, 1997]. In our experience, if all coefficients of variation are small relative to the parameter estimates (we usually judge them favorably if CVs are less than 0.5), the parameters can be considered to be reliably estimated. A final method of judging reliability of estimated parameters is from a calculation of the experimental Damkohler number, $Da1 = (\alpha(1 + A_s/A)L)/V$, where L , the length of the experimental reach, is the only parameter not previously defined. The Damkohler number expresses the relative importance of different solute transport mechanisms (i.e., downstream solute advection compared with solute mass transfer into and out of storage zones). Wagner and Harvey [1997] demonstrated that parameter reliability was greatest (i.e., uncertainty was lowest) in situations where $Da1$ was between 0.01 and 100. $Da1$ values much less than 0.01 indicate situations where relatively little of the tracer mass interacted with storage zones compared to what was advected downstream. Sensitivity to determine storage

parameters in that situation is usually limited. In contrast, $Da1$ values much greater than 100 indicate situations where it is likely that too much interaction occurred between the tracer and storage zones. In those situations the storage parameters are likely to be unidentifiable because of non-uniqueness issues (i.e., tracer data can be simulated equally well either by adjusting the longitudinal dispersion coefficient alone, storage parameters alone, or all of these parameters simultaneously).

4.4. Comparison of Modeling Efficiency Using Zero, One, and Two Storage Zones

[19] To further assess the validity of using a tracer model with storage zones, the results obtained using the OTIS-2Stor module (with two storage zones) were compared with results obtained using the original OTIS model (using first one storage zone and then zero storage zones). As a means to compare the efficiency of the three models in describing the tracer data, we calculated the model selection criterion (MSC), which is based on the Akaike information criterion [Akaike, 1974]. The MSC computes the fraction of the total variance explained by the model but applies a penalty based on the number of optimized parameters. The model with the highest MSC is generally considered to be the most appropriate for describing the experimental data because of the higher information content [Koeppenkastrup and DeCarlo, 1993]. The MSC was calculated as,

$$MSC = \ln \frac{\sum_{i=1}^m w_i [(C_i - C_{av})^2]}{\sum_{i=1}^m w_i [(C_i - c_i)^2]} - \frac{2p}{m}, \quad (4)$$

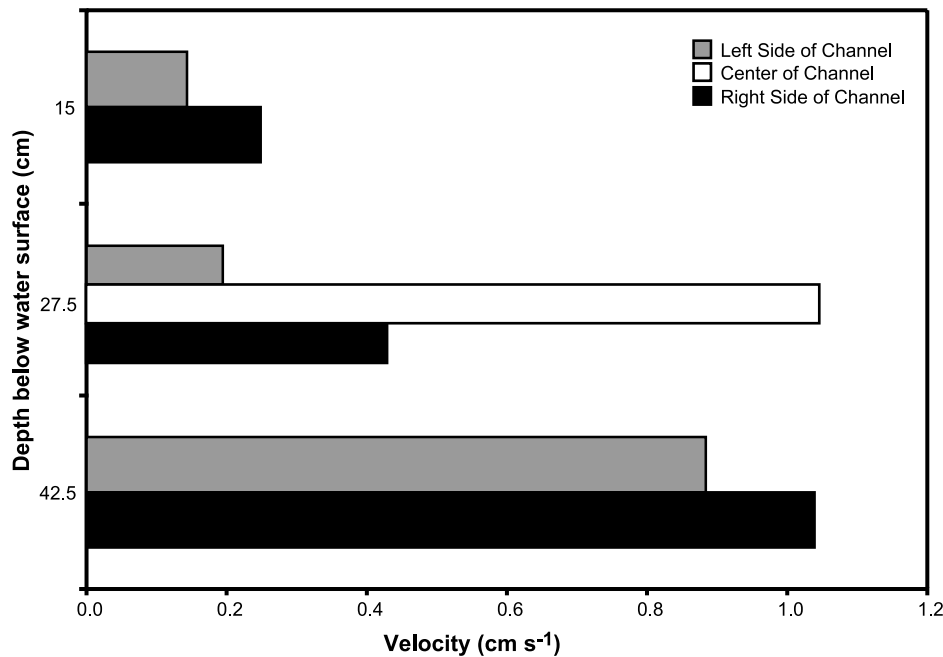


Figure 4. Local horizontal velocities in surface water estimated on the basis of Br tracer travel times to individual sampling tubes shown in Figure 2c. Velocities are grouped by depth of the sampling tube inlets below the water surface. The total depth of the water column was 60 cm.

where i indicates the i th observation of tracer concentration, C_i and c_i are the observed and simulated tracer concentrations, respectively, at the i th observation time, w_i is the weight factor, p is the number of optimized parameters, and m is the total number of observations used in the optimization.

5. Results

5.1. Field Observations

[20] The tracer injection began at 14:15 local time on 20 November 2002. Tracer concentrations at the seven surface water sampling points increased rapidly during the first two hours after the injection started, and then Br concentrations increased more slowly for the next five hours until maximum (plateau) concentrations were reached. After plateaus were reached, Br concentrations fluctuated slowly for the next 15 hours until the tracer was turned off (11:45 on 21 November) (Figure 3). Tracer concentrations on the tail of the breakthrough curve declined rapidly for two hours to a concentration only slightly higher than background, but then those concentrations declined much more slowly for the next 28 hours until concentrations had declined all the way (within the certainty of the measurements) to the background tracer concentration.

[21] Variations in flow velocity with depth in the water column were evident from differences in arrival times of the Br tracer at each sampling tube (Figure 4). Velocities for each sampling tube were computed as the distance from the injection divided by the time at which the tracer reached a concentration equal to 50% of the plateau concentration. Horizontal velocities were slowest (approximately 0.2 cm s^{-1}) in the upper part of the water column, transitional in the middle layer ($0.2\text{--}1.0 \text{ cm s}^{-1}$), and greatest in the lower part of the water column (0.9--

1.0 cm s^{-1}). A single measurement point also was located a small distance (1.8 cm) above the floc. The indicated velocity just above the floc was relatively slow, comparable to the velocity in the upper part of the water column with thick vegetation. Slower velocities near the surface and bottom of the water column probably resulted from greater resistance to flow in the thicker vegetation. Floating in the top 20 cm of the water column was a thick layer of *Utricularia* spp. that could have restricted flow. Tracer was also observed in pore water of the floc and peat up to a distance of 6 cm below the sediment surface. However, the associated velocities were much slower for subsurface flow, with arrival times on the order of hours to tens of hours, compared with arrival times of tens of minutes to hours for the surface water sampling points.

[22] Field data indicated an uneven distribution of bromide across the width of the channel that needed to be evaluated before modeling analysis began. Average Br concentrations on the left side of the channel (viewed downstream) were higher than on the right side. Our interpretation was that the cross-channel pattern in concentration resulted from leakage at the channel sides, which is supported by observations that (1) Br was substantially diluted downstream in the channel such that it was undetectable at a distance of 26 m, (2) plastic sheets that formed the walls of the experimental channel were overlapped at edges rather than sealed and could have allowed leakage, and (3) during the experiment a survey with a Br electrode found Br tracer in the channel to the left (looking downstream) of the experimental channel but not to the right. Leakage apparently occurred as a result of the channel not being perfectly aligned with the regional direction of surface water flow at the time of the experiment, which caused dilution of tracer by inflow of water along the wall on the right side of the channel and outflow of water along the wall on the left side

Table 1. Parameter Values for the Zero-, One-, and Two-Storage Zone Transport Simulations

Parameter	Description	Units	Models ^a		
			Zero-Storage	One-Storage	Two-Storage
Q	volumetric flow rate in channel	$\text{m}^3 \text{s}^{-1}$	6.0E-03	6.0E-03	6.0E-03
$q_L^{\text{in}}, q_L^{\text{out}}$	channel lateral inflow and outflow rate	$\text{m}^3 \text{s}^{-1} \text{m}^{-1}$	9.8E-04	9.8E-04	9.8E-04
D_L	longitudinal dispersion coefficient	$\text{m}^2 \text{s}^{-1}$	5E-05	5E-05	5E-05
A	cross-sectional area (main flow zone)	m^2	0.96 (0.05)	0.92 (0.14)	0.87 (0.14)
A_{S1}	cross-sectional area (storage zone 1)	m^2	–	0.47 (0.36)	0.39 (0.10)
A_{S2}	cross-sectional area (storage zone 2)	m^2	–	–	0.48 (0.48)
α_1	exchange coefficient (storage zone 1)	s^{-1}	–	6.0E-5 (0.64)	1.4E-4 (0.28)
α_2	exchange coefficient (storage zone 2)	s^{-1}	–	–	7.7E-6 (0.21)
t_{S1}	fluid residence time (storage zone 1)	hours	–	2.4	0.89
t_{S2}	fluid residence time (storage zone 2)	hours	–	–	19.9
V	main flow zone velocity	cm s^{-1}	0.63	0.65	0.69
V'	depth-averaged velocity	cm s^{-1}	0.63	0.43	0.34
$Da_{\text{stor } 1}^1$	Damkohler number (storage zone 1)	1	–	0.19	0.45
$Da_{\text{stor } 2}^1$	Damkohler number (storage zone 2)	1	–	–	0.02
MSC	model selection criterion		4.20	4.60	8.73

^aValues in parentheses are coefficients of variation for the parameter estimates determined by nonlinear least squares optimization. Read 6.0E-03 as 6.0×10^{-3} .

of the channel. This pattern of leakage at the walls is consistent with concentrations of tracer that were higher on the left side compared with the right side of the channel.

[23] There was also a vertical trend in the concentration of tracer, with tracer concentrations approximately a factor of 2 higher at the bottom sampling ports compared with the top sampling points. We believe that the vertical gradient in concentration resulted from not having precise control on the individual flow rates to each soaker hose (because tubing was split with y tubing connectors), rather than a problem such as sinking of the tracer in the water column due to density effects. We ruled out density effects because the average velocity of tracer moving across the surface of the soaker hose (calculated from the injection rate, and diameter and total length of soaker hose) was two orders of magnitude lower ($2 \times 10^{-3} \text{ cm s}^{-1}$) than the minimum horizontal velocity measured in the water column ($2 \times 10^{-1} \text{ cm s}^{-1}$). As a result, tracer should have quickly been diluted to a concentration that would have minimized density effects. Also contributing to the mixing of tracer with ambient water were shear effects resulting from flow around the soaker hoses and nearby macrophyte stems. Vertical exchange of water is also known to occur in the Everglades due to the cycle of heating and cooling of the water's surface [Jenter and Schaffranek, 2001], which may also have played a role in mixing the tracer with ambient water. The best explanation for the vertical gradient in tracer concentration therefore is that it resulted from slightly higher tracer flow rates through the lower two soaker hoses. Uneven injection rates would not be expected to affect the average characteristics of advection and longitudinal spreading of the tracer. Significant effects on conclusions from the present experiment are therefore unlikely; however, eliminating this methodological problem from future experiments is advisable.

5.2. Averaging of Tracer Observations for Modeling Analysis

[24] To facilitate a one-dimensional transport analysis, tracer concentrations were averaged across the width and depth of the experimental channel. Arithmetic averaging of concentrations at the seven measurement points might have

been acceptable, but to be certain, we compared arithmetic averages of Br concentrations with flux-weighted averages. Flux weighting considered the percentage of the total cross-sectional area of the channel represented by each sampling tube, as well as the local velocity (Figure 4). We chose to use the flux-weighted series of concentrations for modeling because it is better justified technically and because the weighted concentrations were similar to both the arithmetically averaged concentrations and also to concentrations measured at the center tube in the channel, which lends confidence that conclusions of the experiment are not affected by such decisions.

5.3. Modeling Results

[25] Storage processes in the Everglades were simulated using three models that differed in the number of storage zones involved (zero, one, or two). Final parameter values and their uncertainties are reported in Table 1. All three models used the same values of discharge (Q), inflow and outflow ($q_L^{\text{in}}, q_L^{\text{out}}$), and longitudinal dispersion (D_L). The optimized values of A decreased from the zero- to the one- to the two-storage simulation (from 0.96 to 0.92 to 0.87 m^2). The optimized one-storage model produced a storage zone with a cross sectional area of 0.47 m^2 , while the two-storage simulation produced storage zones with cross sectional areas of 0.39 and 0.48 m^2 , respectively. The best fit exchange parameter determined by optimizing the one-storage model was $6 \times 10^{-5} \text{ s}^{-1}$, which was intermediate between the exchange parameters ($1.4 \times 10^{-4} \text{ s}^{-1}$ and $7.7 \times 10^{-6} \text{ s}^{-1}$) determined for the two-storage simulation. Likewise, optimization of the one-storage model produced an average fluid residence time for its storage zone of 2.4 hours, which was intermediate between the average fluid residence times determined for the two storage zones (0.89 and 19.9 hours). It is worth noting that when expressed per hour, the exchange parameters of the two-storage-zone simulation are equivalent to rates of turnover of main flow zone water (by exchange with storage zones) of 50% and $3\% \text{ h}^{-1}$ respectively.

[26] The average velocity of water flowing in the main flow zone of the water column ($V = Q/A$) was estimated to be 0.69 cm s^{-1} for our experiment. That velocity estimate

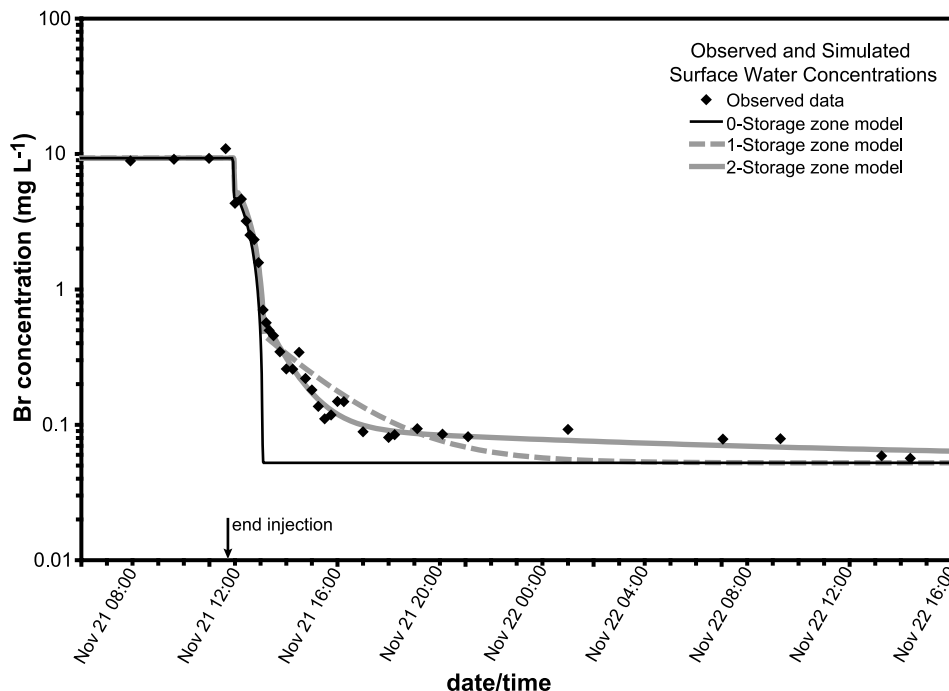


Figure 5. Observed (diamonds) and simulated (lines) concentrations of Br tracer for several hours preceding and for 27 hours following the cutoff of the tracer injection. Parameters for the zero-, one-, and two-storage models are given in Table 1.

is comparable to what would be obtained from other independent measurements of velocity using a technique such as an acoustic Doppler velocity meter. For many purposes, a preferable alternative is to estimate a depth-averaged velocity that represents the entire water column. We refer to that estimate as the “depth-averaged velocity” because it is based on the mean motion of tracer throughout the entire cross section, including tracer that has been delayed by exchange with zones of stagnant or very slow moving water. The depth-averaged velocity, V' , is estimated from the modeling parameters reported in Table 1 as $V' = V \cdot A/(A + A_{s1} + A_{s2})$. The resulting depth-averaged velocity was slower than the main flow zone velocity by approximately a factor of two (0.34 compared with 0.69 cm s^{-1}).

[27] Various indicators suggested that two-storage-zone modeling provided a more precise and less biased (relative to the one-storage simulation) simulation of our Everglades tracer experiment. D_{a1} values were at the low end of the range where reliable results are expected, and parameter uncertainty estimates were typical of a high-quality experiment. Uncertainties are reported in Table 1 as coefficients of variation (i.e., standard deviation of a parameter estimate divided by the parameter value). The parameter that consistently was estimated with the best precision across the zero-, one-, and two-storage models was the cross sectional areas of the main flow zone, A , with CVs of 5%, 14%, and 14%, for zero-, one-, and two-storage models, respectively. The storage parameters α and A_s were more reliably estimated for the two-storage-zone simulation (with CVs ranging from 10–48%) compared with the one-storage simulation (CVs ranging from 36–64%). The poorer fit of the one-storage simulation to tracer data is evident from a visual inspection of model fits.

[28] In contrast to all other parameters, the longitudinal dispersion coefficient, D_L , was estimated with very high uncertainty (CV approximately equal to 10) in the preliminary simulations. The cause appears to have been inadequate sampling frequency at a critical time following the cutoff of the Br tracer injection. An alternative means to estimate longitudinal dispersion was to model the period of rising Br concentrations the previous day. The value of D_L ($5 \times 10^{-5} \text{ m}^2 \text{ s}^{-1}$) that resulted from modeling the rising limb of the tracer experiment turned out to be a close match to the value of D_L ($4 \times 10^{-5} \text{ m}^2 \text{ s}^{-1}$) determined (with much better reliability) from inverse modeling in a fine-particle injection experiment conducted in the same experimental channel a few hours after the Br injection ended [Saiers *et al.*, 2003]. For that reason we felt confident in fixing D_L at a value of $5 \times 10^{-5} \text{ m}^2 \text{ s}^{-1}$ for the final optimization runs using tracer data from the tail of the breakthrough experiments after the Br injection had been turned off (Figure 5).

[29] Accuracy and precision of the simulations were judged visually as well as quantitatively. Judging visually, the two-storage simulation more closely tracked the central tendency of the tracer data compared with the one-storage simulation. The one-storage simulation was biased on the high side of the data early on and then on the low side later in the experiment. Tracer concentrations in the first 5 hours following the cutoff of the tracer injection were consistently overestimated by the one-storage model, followed by the next 19 hours when tracer concentrations were consistently underestimated (Figure 5). The higher value of the model selection criterion (MSC) provides quantitative evidence that the two-storage simulation offers a precise fit to the data (i.e., lower sum of squares of residuals between modeled and observed tracer concentrations) even consid-

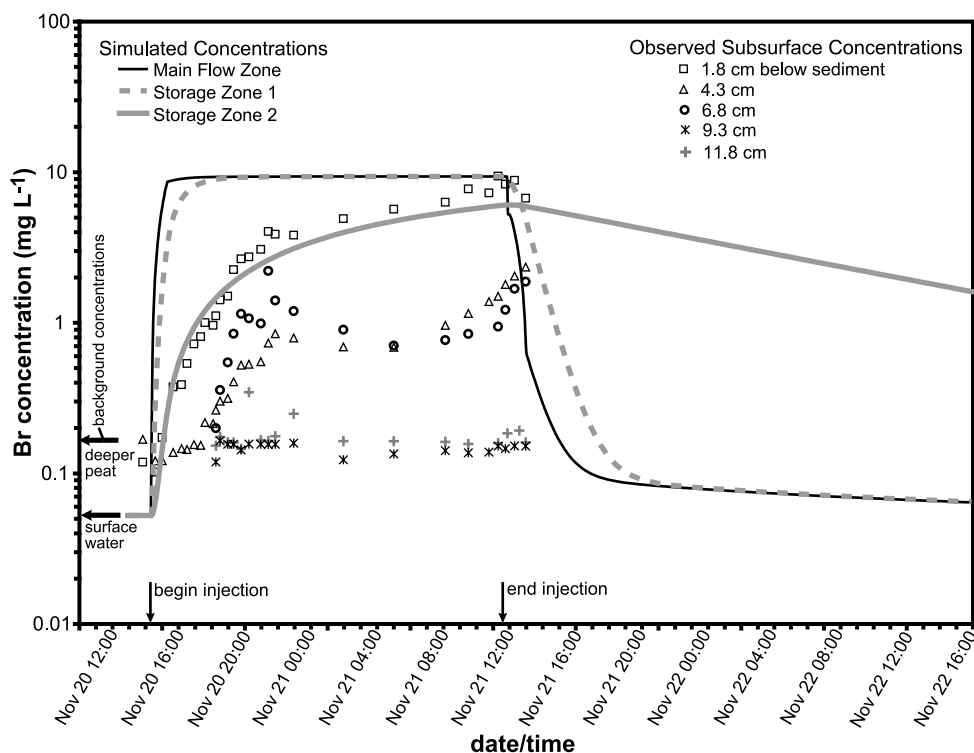


Figure 6. Observed (symbols) concentrations of Br tracer in pore water compared with simulated (lines) concentrations for storage zones 1 and 2 and for the main flow zone in surface water. Simulations are from the two-storage-zone model, using parameter values reported in Table 1. The pore water sampling points are labeled in terms of total depth below the surface of the floc. The total depth of floc is 3 cm, so that the first point (1.8 cm) is located roughly in the center of the floc, the second point is about 1.3 cm into the peat, the third point is 3.8 cm into the peat, etc. The background concentration of Br in deeper pore water (20 and 30 cm) was 0.018 mg L^{-1} .

ering the penalty taken for the greater number of optimized parameters in the two-storage simulation compared with the other models. The last (but not the least important) consideration in our evaluation of models was evaluating the worth of the various models in helping us to partition and quantify the effects of the various physical and biological processes affecting solute transport in Everglades wetlands. All of the quantitative and qualitative criteria presented above suggest that the two-storage model provides a detailed and accurate description of tracer transport in the Everglades without loss of information compared with the parametrically simpler one- and zero-storage models.

5.4. Interpretation of Tracer Storage Mechanisms

[30] Optimizing the model parameters to fit tracer observations was followed by a comparison of the best fit parameters with independently made measurements. The goal was to identify the mechanisms of storage, beginning with an interpretation of the characteristics of the main flow zone. The parameters determined by inverse modeling describe a main flow zone that is similar to direct measurements of flow velocity in the open part of the water column beneath the *Utricularia* canopy. For example, the model estimated velocity in the main flow zone (0.69 cm s^{-1}) was intermediate between measured velocities in the middle (0.54 cm s^{-1}) and lower (0.95 cm s^{-1}) parts of the water column compared with the measured velocity in the

Utricularia canopy (0.2 cm s^{-1}). Also, the model estimated cross sectional area of the main flow zone (approximately 0.87 m^2) accounted for only about half of the measured area of open water column (1.8 m^2) in the experimental channel.

[31] Model estimated parameters for storage zone 1 appear to have accounted for water exchange between the main flow zone and more slowly flowing water in the *Utricularia* layer. In particular, the similarity in transport timescales and thicknesses of the *Utricularia* layer and storage zone 1 permit the interpretation that storage zone 1 provides a model for the effects of the *Utricularia* layer on transport through the wetland. Dividing the distance (6.8 m) by that velocity yields approximately a 1 h travel time through the *Utricularia* layer, which is broadly consistent with the average fluid residence time (0.89 h) determined for storage zone 1 by tracer modeling. In addition to comparing residence times, the measured depth of the *Utricularia* layer can also be compared with the modeled depth of storage zone 1. The maximum measured depth of the *Utricularia* layer (20 cm) was somewhat thicker than the modeled depth of storage zone 1 (13 cm). However, the density of *Utricularia* was observed qualitatively to decrease with depth in the water column, and it is possible that the modeling was sensitive to a shallower “effective” depth of *Utricularia* rather than a maximum depth.

[32] The average fluid residence time of storage zone 2 (19.9 h) was more than an order of magnitude greater than that of storage zone 1. Because the relative sizes of the two

storage zones differed very little, their vastly different fluid residence times indicate much slower exchange between the main flow zone and storage zone 2. Our interpretation is that storage zone 2 was sensitive to solute exchange with pore water in the floc and shallow peat. That interpretation is based on a comparison of modeled storage zone concentrations and measurements of tracer measurements made in situ in the pore water. Tracer concentrations measured within the floc and shallow peat indicate that bromide moved a total distance of approximately 6 cm into the subsurface on a timescale of tens of hours (Figure 6). Although these measurements are difficult to compare directly with modeled tracer concentrations for storage zone 2 (because modeled concentrations represent an average that assumes complete mixing in the storage zone), the timescale of hours to tens of hours for buildup of tracer concentrations in the subsurface is broadly consistent with a storage zone 2 residence time of approximately 20 h.

[33] A discrepancy exists, however, between the measurements and modeling of the size of storage zone 2, with the modeled depth of storage zone 2 (16 cm) being more than twice the depth (6 cm) of measured bromide penetration into floc and peat. The discrepancy in storage depth might be explained by a relatively high uncertainty in the modeled cross-sectional area for storage zone 2. The coefficient of variation for A_{s2} (49%) was at least 3 times greater than the coefficients of variation for the other storage parameters of the two-storage model (which did not exceed 16%). Another possible explanation is that some of the long-timescale storage characterized by storage zone 2 occurred elsewhere, such as water near the surface or water in the bottom few centimeters next to the bed. Both of those environments have periphyton or epiphyton present that could participate in storage. Although no tracer samples were collected in the top few centimeters of the surface water, we suspect that storage on the timescale of tens of hours occurred there. Storage on the order of tens of hours might also have occurred in surface water very close to the sediment bed, where bed roughness and thicker stems of macrophytes may also have locally increase resistance to flow. These observations suggest that while storage zone 2 predominantly characterized subsurface storage, also characterized were small zones of relatively long-timescale storage in periphyton (near the water's surface) and in surface water and thick epiphyton layers on macrophyte stems near the sediment bed.

6. Discussion

[34] The justifications for simulating solute transport in the Everglades using a model with two storage zones includes greater precision of parameters estimates and less bias in the simulation compared with the one-storage-zone model. The major problem of the one-storage-zone model is that it could not simultaneously describe both the short (timescale of minutes to hours) and much longer (timescale of hours to tens of hours) behavior of storage. The two-storage-zone model not only provided a means to more accurately simulate tracer data, but also afforded the opportunity to interpret the mechanisms of storage. Comparison of storage zone sizes and fluid residence times from the two-storage model with independently collected data showed the importance of zones of thick floating vegetation

and zones in peat pore water in delaying the downstream movement of tracer. Our results therefore were helpful in helping to identify the causes of storage in the Everglades. Specifically, the role that key physical features such as floating vegetation and peat pore water play in slowing the downstream movement of solute was quantified. This type of information will ultimately be used to increase our understanding about the interactions between physical and biological processes that control the fate of nutrients and contaminants in the Everglades.

6.1. Depth-Averaged Velocity Estimate

[35] An important outcome of our tracer experiment was to demonstrate that solute velocities in the Everglades are slower than estimates based on alternative velocity measurements that are employed only in the open part of the water column. Alternative measurements of velocity (including Doppler-based techniques) will tend to overestimate solute velocities in the Everglades because they cannot observe water movement through zones of thick vegetation such as submersed floating plants or movement of pore water through peat. Differences in velocity estimates are illustrated by the following comparison. Velocity in the main flow zone (where flow was relatively unobstructed) was estimated to be 0.69 cm s^{-1} in our experiment, using the calculation $V = Q/A$, where A represents only the cross sectional area of the main flow zone. That approach to estimating velocity is comparable to what would be obtained from averaging several measurements of velocity determined in the open part of the water column using a technique such an acoustic Doppler measurement technique. For many purposes, a preferable alternative would be estimating a velocity representing the entire water column. A fully depth-averaged estimate of velocity is possible using our tracer results, and is referred to as the "depth-averaged velocity" because it is based on the mean motion of tracer through the entire cross section, including tracer that is exchanged with stagnant or very slowly moving water in thick vegetation or in the subsurface. The depth-averaged velocity is estimated as $V' = V \cdot A/(A + A_{s1} + A_{s2})$. The depth-averaged tracer velocity V' was slower than the main flow zone velocity V by approximately a factor of 2 (0.34 compared with 0.69 cm s^{-1}). The difference between the tracer velocity and the main flow zone velocity is explained by the large fraction of the cross sectional area in the Everglades wetland (i.e., $(A_{s1} + A_{s2})/A \approx 1.0$) that participates in storage and the prolonged residence times of water in those storage zones (Table 1). Identifying which physical and/or biological features participate in storage required additional measurements of tracer breakthrough. Those additional tracer measurements allowed us to identify the independent roles of storage in the floating layer of *Utricularia* and in shallow subsurface flow paths through floc and peat.

6.2. Longitudinal Mixing Estimates in the Everglades

[36] Surface flow in the Everglades is thought to be laminar under most conditions [Lee *et al.*, 2004]. The relevant criterion is the stem Reynolds Number ($Re_d = Vd/\nu$), where V is the average velocity, ν is the kinematic viscosity, and d is stem diameter. The stem Reynolds Number was approximately 12 for our experiment, which is well below the threshold for fully developed turbulent

flow ($Re_d = 200$) or onset of the formation of vortex shedding wakes behind stems ($Re_d = 50$). Turbulence was therefore not a factor controlling longitudinal mixing of solutes in our tracer experiment. These criteria for turbulence in wetlands were established in laboratory flumes containing model vegetation and in field experiments [Leonard and Luther, 1995; Nepf, 1997; Nepf, 1999]. Other processes potentially contributing to longitudinal mixing in the Everglades include shear flow at the sediment bed and mechanical dispersion resulting from flow around stems [Nepf, 1999; Saiers et al., 2003], overturn of the water column and vertical mixing of solutes driven by thermal effects [Jenter and Schaffranek, 2001], vertical exchange of solutes between differently vegetated layers in the water column (this study), and vertical exchange between surface water and subsurface pore water (this study).

[37] A goal of the present project was to interpret the modeling results in terms of the actual wetland processes involved, and, when possible, to group the processes that are causing longitudinal mixing with the specific terms that represent the mixing in the model. Several terms in the model potentially can characterize longitudinal mixing of solutes. Because the modeling itself is not specific about the mixing processes involved, the different modeling terms only vary functionally in their timescale. Relatively fast components of mixing in the open part of the water column were expected to be accounted for through the specification of the longitudinal dispersion parameter, whereas the slower mixing processes were expected to be accounted for through specification of storage zone cross-sectional areas and exchange rates.

[38] When summed, the cross sectional areas of the main flow zone and the two storage zones (0.39 and 0.48 m², respectively) accounted for 97% of the total wetted cross section in the experimental channel. The “main flow zone” had an estimated cross sectional area of approximately 0.87 m², which accounts for approximately half of the total wetted cross section in the experimental channel (1.8 m²). Our overall interpretation was that the model’s main flow zone characterized advection that occurred in the middle of the water column where flow was restricted only by macrophyte stems and not by the floating *Utricularia* or by the bottom irregularities and greater stem densities near the bottom of the water column. The relatively rapid solute mixing processes (i.e., the ones that established an equilibrium rate of mixing faster than the mean arrival time at the monitoring site), were characterized by the longitudinal dispersion coefficient, which was hypothesized to characterize the effects of velocity variations due to flow around macrophyte stems in the main flow zone. Slower mixing processes were hypothesized to have resulted from solute exchange with (1) water within the upper part of the floating mat of *Utricularia* sp., (2) shallow pore water in floc and peat, and (3) water in the bottom few or top few centimeters of the water column, where velocities were slowed by bed shear and/or greater stem densities and epiphyton. What follows is a discussion of the independent measurements that were made and various other pieces of information that help support or contradict these hypotheses.

[39] Mixing due to mechanical dispersion around stems was likely to be important in affecting longitudinal dispersion, because plant stem density and average stem diameter

were large enough to cause significant mechanical dispersion according to the criteria of Nepf [1999]. The fraction of the water column occupied by macrophyte stems (0.013) was calculated using the average stem diameter (0.2 cm) and the average number of macrophyte stems per area (1147 m⁻²) (D. Lee and A. Edwards, unpublished data, 2004). Another metric is the frontal area of stems per volume, which is estimated as the fractional volume of stems divided by average stem diameter. Frontal area of macrophyte stems per volume averaged 0.065 cm⁻¹ in our experiment. Using equation (7b) of Nepf [1999], we conservatively estimated a mechanical dispersion coefficient for our experiment to be on the order of 10⁻⁷ m² s⁻¹, which is two orders of magnitude lower than our estimated longitudinal dispersion coefficient determined by our inverse modeling (5 × 10⁻⁵ m² s⁻¹). The estimate for mechanical dispersion is conservative because it does not account for the possible effects of heterogeneities in stem spacing in increasing longitudinal dispersion. Using our experimentally determined estimate of longitudinal dispersion ($D_L = 10^{-5}$ m² s⁻¹), we estimated (using the calculation D_L/V) that the scale of heterogeneities controlling longitudinal dispersion is on the order of 1 cm. The suggestion that longitudinal dispersion results from velocity variability at the scale of centimeters is consistent with a control by heterogeneities in the spacing between macrophyte stems, for which the mean spacing was estimated by the calculation given by Nepf [1999] to be approximately 2 cm. Mechanical dispersion around individual macrophyte stems is therefore most likely a minor determinant of longitudinal dispersion, with larger, centimeter-scale heterogeneities in stem spacing appearing to be the more important control.

[40] As noted earlier in this paper, flow was approximately a factor of 5 slower in the top 20 cm of the water column due to greater resistance to flow through the layer of floating vegetation, *Utricularia*. We did not quantify the density of *Utricularia* spp. at our site, but estimates of *Utricularia* biomass (62 g dry weight m⁻²) and wet density data (1 g cm⁻³) data were available from another investigator working at a nearby site (Greg Noe, personal communication). The estimated volume fraction of *Utricularia* (0.031) and frontal area (0.78 cm⁻¹) were substantially larger than for the macrophytes. An estimated average stem diameter (0.04 cm) was determined from a scale drawing of *Utricularia*.

[41] The measurements of Br movement into the subsurface leave little doubt that surface-subsurface exchange occurs in the Everglades. Still, uncertainties remain about the rates of movement and the causes. Although the method of pumping slowly (1.5 mL min⁻¹ for about 10% of the time) and collecting small sample volumes (10 mL) for tracer analysis has been proven in streams [Duff et al., 1998; Harvey and Fuller, 1998], there may be as yet unforeseen difficulties in wetlands. More work of this type should help prove the reliability of the technique. With regard to driving forces for subsurface transport of solutes, diffusion can only account for a small portion of the observed transport of the Br tracer into pore water. A mean distance for diffusive transport of bromide into the peat was estimated based on $L = \sqrt{tD_s}$, where D_s is the sedimentary diffusion coefficient, L is the transport distance, and t is time [Lerman, 1979]. The sedimentary diffusion coefficient for bromide

was estimated from the bromide diffusion coefficient in free water multiplied by the sediment porosity squared, a term that scales diffusion to account for porosity and tortuosity effects in sediment [Lerman, 1979]. Using the resulting estimate of the sedimentary diffusion coefficient ($1.5 \times 10^{-5} \text{ cm}^2 \text{ s}^{-1}$), the mean transport distance into the sediment over a 24 hour period was estimated to be approximately 1.2 cm in 24 hours. With diffusion discounted, exchange across the sediment surface might also be caused by horizontal advection through the hummocky features on the wetland surface, which could conceivably explain penetration as deep as the average size of the bed forms. In our case, microtopographic measurements of the surface elevation indicate a standard deviation of ground surface elevations of approximately 3 cm, suggesting that horizontal advection through bed forms can explain, at most, approximately one half of the observed transport into the sediment. Other possible driving forces are hydraulic gradients associated with groundwater recharge or root water uptake by macrophytes associated with evapotranspiration. Elucidation of the mechanism driving solute into subsurface storage zones is a priority for future investigations.

6.3. Summary

[42] A 22 h injection of a conservative solute tracer was conducted in Everglades' surface water. A key result was that the average velocity with which solute moves through the surface water system (0.34 cm s^{-1}) was retarded by a factor of approximately 50% compared to the mean velocity of flow in the relatively "open" part of the water column (0.69 cm s^{-1}) where only emergent macrophyte stems were present. The reduction in average depth-averaged velocity relative to velocity in the main flow zone could not have been determined with commonly used velocity measuring devices in wetlands, such as acoustic Doppler flowmeters, because those methods are generally only reliable in the open part of the water column. The reduction in the rate of solute transport was due to exchange that occurs with relatively slow moving or stagnant water in floating vegetation, and in pore water of floc and peat. On the basis of all evidence we tentatively conclude that storage zone 1 predominantly characterized solute exchange between the main flow zone and the thick floating mat of *Utricularia* spp., while storage zone 2 predominantly characterized surface-subsurface exchange with pore water in floc and peat in our Everglades tracer experiment.

[43] Our transport experiment was designed to quantify the storage processes that result in a reduction of the average velocity and longitudinal mixing of solutes. The fastest timescale of mixing was characterized as a longitudinal dispersion coefficient (value of $5 \times 10^{-5} \text{ m}^2 \text{ s}^{-1}$) which characterized mixing processes on the timescale of minutes to tens of minutes). Longitudinal dispersion appeared to be associated with mechanical dispersion resulting from the laminar flow of surface water around heterogeneously distributed stems of macrophytes (predominantly *Eleocharis* spp.). An intermediate timescale of mixing was characterized by a model storage zone with an approximate thickness of 13 cm and a fluid residence time of 1 h, which was interpreted to be the result of solute exchange between a main flow zone in the bottom two thirds of the water column where only macrophyte stems were present, and a layer of thick floating vegetation

(predominantly *Utricularia* sp.) in the top third of the water column. The longest timescale of solute mixing was characterized by a model storage zone with an approximate thickness of 16 cm and a fluid residence time of approximately 20 h, which characterized solute exchange with pore water flowing through the underlying floc and peat sediment, and also possibly the boundary layer waters just above the sediment and just beneath the surface of the water column.

[44] Increased understanding of these storage processes is important for several reasons. Storage environments in the wetlands cause dispersion and delay of solutes moving through the Everglades landscape. Storage zones are likely also to be locations of enhanced biogeochemical reactions, which could have substantial effects on water quality in the Everglades. Future research could focus on more definitive identification of storage processes and how to parameterize them based on physical principles, and also on the inclusion of reactive transport processes in order to investigate the combined effects of physical transport and chemical reaction on water quality in the Everglades and in other wetlands.

[45] **Acknowledgments.** This work was funded by the U.S. Geological Survey's Priority Ecosystem Program and by the U. S. Geological Survey's National Research Program. We are indebted to Evelyn Gaiser and Christine Taylor for granting permission and providing access to the flume facility and for general assistance regarding the experiments. We also are grateful to Jim Krest, Steve Mylon, and Lisbet Kugler for their steadfast assistance in fieldwork, and to Mike Gooseff and two anonymous reviewers who supplied helpful comments through the review process at WRR.

References

- Akaike, H. (1974), A new look at the statistical model identification, *IEEE Trans. Autom. Control*, *19*, 716–723.
- Andradottir, H. O., and H. M. Nepf (2001), Impact of exchange flows on wetland flushing, *Water Resour. Res.*, *37*(12), 3265–3273.
- Bates, A. L., W. H. Orem, J. W. Harvey, and E. C. Spiker (2002), Tracing sources of sulfur in the Florida Everglades, *J. Environ. Qual.*, *31*, 287–299.
- Choi, J., J. W. Harvey, and M. H. Conklin (2000), Characterizing multiple timescales of stream and storage zone interaction that affect solute fate and transport in streams, *Water Resour. Res.*, *36*(6), 1511–1518.
- Donaldson, J. R., and P. V. Tryon (1990), User's guide to STARPAC, The Standards Time Series and Regressions Package, *Internal Rep. NBSIR 86-3448*, Natl. Inst. of Stand. and Technol., Boulder, Colo.
- Duff, J. H., F. Murphy, C. C. Fuller, F. J. Triska, J. W. Harvey, and A. P. Jackman (1998), A mini drivepoint sampler for measuring porewater solute concentrations in the hyporheic zone of sand-bottom streams, *Limnol. Oceanogr.*, *43*(6), 1378–1383.
- Gooseff, M. N., D. M. McKnight, R. L. Runkel, and J. H. Duff (2004), Denitrification and hydrologic transient storage in a glacial meltwater stream, McMurdo Dry Valleys, Antarctica, *Limnol. Oceanogr.*, *49*(5), 1884–1895.
- Harvey, J. W., and C. C. Fuller (1998), Effect of enhanced manganese oxidation in the hyporheic zone on basin-scale geochemical mass balance, *Water Resour. Res.*, *34*(4), 623–636.
- Harvey, J. W., and B. J. Wagner (2000), Quantifying hydrologic interactions between streams and their subsurface hyporheic zones, in *Streams and Ground Waters*, edited by J. A. Jones and P. J. Mulholland, pp. 3–44, Elsevier, New York.
- Harvey, J. W., R. M. Chambers, and J. R. Hoelscher (1995), Preferential flow and segregation of porewater solutes in wetland sediment, *Estuaries*, *18*(4), 568–578.
- Harvey, J. W., S. L. Krupa, and J. M. Krest (2004), Ground water recharge and discharge in the central Everglades, *Ground Water*, *42*(7), 1090–1102.
- Jenter, H. J., and R. W. Schaffranek (2001), Observations of daily temperature patterns in the southern Florida Everglades, paper presented at Wetlands Engineering and River Restoration Conference, Am. Soc. of Civ. Eng., Reno, Nev., 27–31 Aug.

- Jones, J. B., and P. J. Mulholland (2000), *Streams and Ground Waters*, Elsevier, New York.
- Jones, R. D., J. Trexler, and D. L. Childers (1999), Numerical interpretation of class III narrative nutrient water criteria for Everglades wetlands: Annual report 1999, Southeast Environ. Res. Cent., Fla. Int. Univ., Miami.
- Kadlec, R. H., and R. L. Knight (1996), *Treatment Wetlands*, CRC Press, Boca Raton, Fla.
- Keefe, S. H., L. B. Barber, R. L. Runkel, J. N. Ryan, D. M. McKnight, and R. D. Wass (2004), Conservative and reactive solute transport in constructed wetlands, *Water Resour. Res.*, 40, W01201, doi:10.1029/2003WR002130.
- Koeppenkastrop, D., and E. H. DeCarlo (1993), Uptake of rare earth elements from solution by metal oxides, *Environ. Sci. Technol.*, 27, 1796–1802.
- Krabbenhof, D. P., J. P. Hurley, M. L. Olson, and L. B. Cleckner (1998), Diel variability of mercury phase and species distributions in the Florida Everglades, *Biogeochemistry*, 40, 311–325.
- Lee, J. K., L. C. Roig, H. L. Jenter, and H. M. Visser (2004), Vertically averaged flow resistance in free surface flow through emergent vegetation at low Reynolds numbers, *Ecol. Eng.*, 22, 237–248.
- Leonard, L. A., and M. E. Luther (1995), Flow hydrodynamics in tidal marsh canopies, *Limnol. Oceanogr.*, 40, 1474–1484.
- Lerman, A. (1979), *Geochemical Processes: Water and Sediment Environments*, John Wiley, Hoboken, N. J.
- Martinez, C. J., and W. R. Wise (2003), Analysis of constructed treatment wetland hydraulic with the transient storage model OTIS, *Ecol. Eng.*, 20, 211–222.
- McClain, M. E., et al. (2003), Biogeochemical hot spots and hot moments at the interface of terrestrial and aquatic ecosystems, *Ecosystems*, 6(4), 301–312, doi:10.1007/s10021-003-0161-9.
- National Research Council (2003), *Does Water Flow Influence Everglades Landscape Patterns?*, Natl. Acad. Press, Washington, D. C.
- Nepf, H. M. (1997), The effects of vegetation on longitudinal dispersion, *Estuarine Coastal Shelf Sci.*, 44, 675–684.
- Nepf, H. M. (1999), Drag, turbulence, and diffusion in flow through emergent vegetation, *Water Resour. Res.*, 35, 479–489.
- Noe, G. B., D. L. Childers, A. L. Edwards, E. Gaiser, K. Jayachandran, D. Lee, J. Meeder, J. Richards, L. J. Scinto, J. C. Trexler, and R. D. Jones (2002), Short-term changes in phosphorus storage in an oligotrophic Everglades wetland ecosystem receiving experimental nutrient enrichment, *Biogeochemistry*, 59(3), 239–267.
- Riscassi, A. L., and R. W. Schaffranek (2003), Flow velocity, water temperature, and conductivity in Shark River Slough, Everglades National Park, Florida: August 2001–June 2002, *U.S. Geol. Surv. Open File Rep.*, 03-348.
- Runkel, R. L. (1998), One-dimensional transport with inflow and storage (OTIS): A solute transport model for streams and rivers, *U.S. Geol. Surv. Water Resour. Invest. Rep.*, 98-4018.
- Saiers, J. E., J. W. Harvey, and S. E. Mylon (2003), Surface-water transport of suspended matter through wetland vegetation of the Florida Everglades, *Geophys. Res. Lett.*, 30(19), 1987, doi:10.1029/2003GL018132.
- Schulz, R., and S. K. Peall (2001), Effectiveness of a constructed wetland for retention of nonpoint-source pesticide pollution in the Lourens River catchment, South Africa, *Environ. Sci. Technol.*, 35, 422–426.
- Tobias, C. R., S. A. Macko, I. C. Anderson, E. A. Canuel, and J. W. Harvey (2001), Tracking the fate of a high concentration groundwater nitrate plume through a fringing marsh: A combined groundwater tracer and in situ isotope enrichment study, *Limnol. Oceanogr.*, 46(8), 1977–1989.
- Wagner, B. J., and J. W. Harvey (1997), Experimental design for estimating parameters of rate-limited mass transfer: Analysis of stream tracer studies, *Water Resour. Res.*, 33(7), 1731–1741.
-
- J. W. Harvey and J. T. Newlin, U.S. Geological Survey, Reston, VA 20192, USA. (jwharvey@usgs.gov)
- J. E. Saiers, School of Environmental Studies, Yale University, New Haven, CT 06521, USA.